Nov 7th, 12:00 AM - Nov 8th, 12:00 AM

Flexural Strength of Continuous-Span Z-Purlins with Paired Torsion Braces using the Direct Strength Method

Michael Seek

Wei-Wen Yu International Specialty Conference on Cold-Formed Steel Structures
St. Louis, Missouri, U.S.A., November 7 & 8, 2018

Flexural Strength of continuous-span Z-purlins with paired torsion braces using the Direct Strength Method

Michael W. Seek[1]

Abstract

A procedure is presented to calculate the local and distortional flexural buckling strength of continuous span purlins with paired torsion braces using the Direct Strength Method. Displacement compatibility is utilized to determine the forces interacting between the purlin, the flexible diaphragm and the torsion braces. The biaxial bending and torsion effects caused by this interaction are superimposed, and the actual distribution of stresses within the cross section are calculated at critical locations along the span. With this distribution of stresses, a finite strip buckling analysis is performed to determine the local and distortional buckling strength. In current design practice, results from a simple span Base Test are extrapolated to multi-span systems using a constrained bending stress distribution. In previous work, a variation of the presented method was compared to simple span base test results with good correlation. In this paper, the simple span stresses are compared to the stresses of continuous span systems. Significant, although typically conservative differences in the stress distributions and, as a result the predicted flexural strength, are observed in the comparison between simple span and multi-span systems. Additionally, significant changes in the distribution of stresses are observed as roof slope effects are considered. Increases in the flexural strength with increasing roof slope are reported and compared to the strength predicted by the current base test method.

Introduction

In the United States, purlins with one flange attached to standing seam sheathing are designed according to the Base Test Method (AISI 2013). According to this method, the purlin system is tested in a vacuum chamber in a simple span configuration to determine the nominal flexural strength. While the standing seam sheathing provides lateral and torsional restraint to the purlin, this restraint

[1] Associate Professor, Old Dominion University, Norfolk, VA USA

is very flexible. Attempts to analytically calculate the flexural strength have been generally unsuccessful and thus the need of the industry to rely on the Base Test Method. With the Base Test Method, a reduction factor, R, determined from the base test is applied to account for the flexibility of the restraint provided by the sheathing. The nominal flexural strength, M_n, of the purlin is then calculated from the AISI Specification Appendix A Section I6.2.2 (AISI 2016)

$$M_n = R \cdot M_{n\ell o} \tag{1}$$

where $M_{n\ell o}$ is the nominal flexural strength considering local buckling only with a constrained bending stress distribution.

Although the Base Test is performed on a flat-slope, simple-span specimen, extensive testing at Virginia Tech (AISI 2013) showed that the results of the base test could be conservatively extrapolated to multi-span roof systems. To account for slope effects, external anchors must be designed to resist downslope forces. The Base Test must be representative of the conditions in the field, therefore, if modifications to the system are desired, additional base testing is required.

A method to predict the flexural strength of purlins with paired torsion braces was first presented by Seek et. al. (2016) and further modified by Seek and Parva (2018). The methodology considers displacement compatibility between the purlin, standing seam sheathing, and the paired torsion braces to determine the interacting forces between the components. By superimposing these interacting forces with the externally applied system forces, the true distribution of stresses on the cross section can be determined. This distribution of stresses considers the biaxial bending stresses caused by a flexible diaphragm and the distribution of torsion stresses that result from torsion along the span of the purlin. Additionally, because these systems can be very flexible, the methodology approximates additional second order stresses that may be introduced. With this true distribution of stresses, a finite strip buckling analysis is performed to determine the local and distortional buckling strength.

Seek and Parva (2018) compared this methodology to a series of base tests and found good correlation between the tested strength and predicted strength. Additionally, the methodology was able to predict and provide rationale for some anomalies in the tests: flexural buckling failures away from the mid-span at the brace location, and failures varying between upslope purlin and downslope purlin in the tests.

Because most purlin roof systems are designed as continuous, the methodology is expanded herein to account for bending continuity and roof slope. For the equation development, continuous systems are approximated with rigidly fixed ends. To demonstrate the methodology and to highlight the variation in predicted strength when compared to the base test method, purlin strength is calculated at several roof pitches.

Calculating cross section stresses

Displacement compatibility is utilized to determine the forces interacting between the purlin, standing seam sheathing, and torsion braces. Lateral displacement compatibility between the purlin and sheathing is determined at the torsion brace location. Similarly, torsion rotation compatibility between the purlin and the torsion braces is determined at the location of the torsion brace. In this formulation of torsion compatibility, the torsion braces are considered to be rigid and the torsion restraint provided by the sheathing is ignored. In most cases, this approach is conservative.

The first step in the process is to determine the horizontal restraining force in the diaphragm, w_{rest}, that results from the unsymmetric bending of the purlin and the downslope forces on the sloped roof. Previously developed equations by Seek and Parva, used the symbol, σ, to represent the proportion of the *gravity* load that was translated into an in-plane force in the diaphragm. For sloped roof systems, it is more appropriate to define the in-plane force in the diaphragm relative to the applied force *perpendicular* to the plane of the sheathing. To highlight this subtle distinction, the terminology was changed such that the term, ρ, represents the proportion of the force applied perpendicular to the plane of the sheathing that results in an in-plane force in the diaphragm. Therefore uniform force in-plane force in the diaphragm is

$$w_{rest} = w\left(\cos\theta\right)\rho \tag{2}$$

where w is the uniformly applied load in the gravity direction and

$$\rho = \frac{C_1 \dfrac{\left(\dfrac{I_{xy}}{I_x}\right)L^4}{EI_{my}} + C_2 \dfrac{L^2 \tan\theta}{G'spa}}{C_1 \dfrac{L^4}{EI_{my}} + C_2 \dfrac{L^2}{G'spa}} \tag{3}$$

In Eq. (3), L is the span of the purlin, G' is the stiffness of the diaphragm, spa is the depth of the diaphragm tributary to the purlin (generally the purlin spacing), I_{my} is the modified moment of inertia about the orthogonal y-axis as defined by Zetlin and Winter (1955), and coefficients C_1 and C_2 are derived from displacement compatibility.

$$C_1 = \frac{1}{24} \cdot \left(\frac{c}{L}\right)^2 \cdot \left(1 - \frac{c}{L}\right)^2 \tag{4}$$

$$C_2 = \frac{1}{2} \cdot \left(\frac{c}{L}\right) \cdot \left[1 - \left(\frac{c}{L}\right)\right] \tag{5}$$

In the above equations, c is the distance from the end of the span to the location of the torsion brace.

Accurately quantifying the horizontal restraining force of the diaphragm is important because it has a large impact on the torsion along the length of the purlin. Because the horizontal restraining force is applied at an eccentricity relative to the shear center of the purlin, e_{sy}, it imparts a uniform torsion along the purlin. This eccentricity should include the effective standoff, s, of the clip connection between the purlin and sheathing as shown in Figure 1 and defined by Seek and McLaughlin (2017). The uniform torsion from the horizontal diaphragm restraint is combined with the torsion caused by the eccentricity, e_{sx}, of load applied perpendicular to the plane of the sheathing to create a net uniform first order torsion, t_{1st}, where

$$t_{1st} = \left(w \cdot \cos\theta\right)\left(\rho \cdot e_{sy} - e_{sx}\right) \tag{6}$$

The restraining force in the diaphragm is also used to define the mid-span lateral displacement of the purlin relative to the support location, Δ_{mid}, where

$$\Delta_{mid} = w\left(\rho\cos\theta - \sin\theta\right)\frac{L^2}{8G'\left(spa\right)} \tag{7}$$

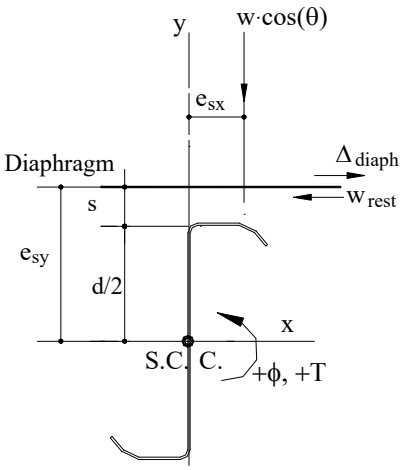

Figure 1. Axes and positive force directions

The lateral displacement is positive for an upslope translation and negative for downslope translation. The lateral displacement of the purlin relative to the supports causes a second order torsion with a parabolic distribution. The peak torsion at mid-span, t_{2nd} is

$$t_{2nd} = -\left(w \cdot \cos\theta\right)\Delta_{mid} \tag{8}$$

The torsion introduced along the length of the purlin is resisted at the brace locations. Displacement compatibility between the purlin and the brace, assuming a rigid brace, is enforced at the brace location to determine the magnitude of the brace forces. Because purlin torsion behavior is dominated by warping torsion, the balance of torsion eliminates consideration of pure torsion which greatly simplifies the equations and results in negligible difference in the calculated results. The brace torque resulting from the first order uniformly distributed torsion, T_{1st}, is

$$T_{1st} = -C_3 t_{1st} L \tag{9}$$

where

$$C_3 = \frac{1}{4} \cdot \frac{\left(1 - \frac{c}{L}\right)^2}{\left(\frac{c}{L}\right)\left(2 - 3\frac{c}{L}\right)} \tag{10}$$

The brace torque from the second order effects with a parabolic load distribution, T_{2nd}, is

$$T_{2nd} = -C_4 t_{2nd} L \tag{11}$$

where

$$C_4 = \frac{1}{15} \cdot \frac{3 - 5\left(\frac{c}{L}\right) + 3\left(\frac{c}{L}\right)^3 - \left(\frac{c}{L}\right)^4}{2\left(\frac{c}{L}\right) - 3\left(\frac{c}{L}\right)^2} \tag{12}$$

Because paired torsion braces are often not anchored externally, to balance the restraining torque at each end of the brace, a shear force, V, is generated at each end of the brace as shown in Fig. 2.

$$V = \frac{2\left(T_{1st} + T_{2nd}\right)\xi}{spa} \tag{13}$$

Where $\xi = 1$ for the downslope purlin and -1 for the upslope purlin.

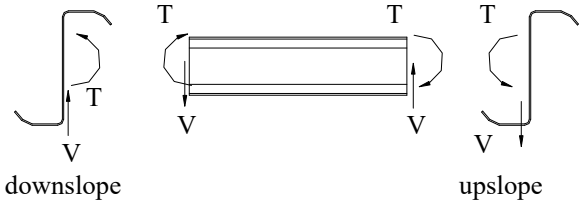

Figure 2. Shear forces to balance brace moment

For flexible standing seam diaphragms, at low slope, the system of purlins translates laterally upslope. The second order torsion induced by this displacement dominates, causing an uphill rotation of the purlin. The moment generated in the torsion braces as they resist this rotation of the purlin is directed as shown in Fig. (2). The shear force acts downward on the upslope purlin, increasing the moment about the x-axis in the purlin by as much as 20%. Correspondingly, downslope purlin will experience a decrease in the moment about the x-axis. As a result, for identical purlins, the upslope purlin will be the first to fail. As the slope of the roof increases, the second order torsion is reduced, and the resisting moment in

the brace will reverse directions. Correspondingly, the shear force will reverse directions, and the downslope purlin will become critical.

Upon defining the magnitude and direction of the additional shear force generated at the brace, the bending normal stresses can be determined. For simplicity, forces are oriented along the orthogonal x- and y- axes perpendicular and parallel to the web respectively. There are 3 contributions to the bending stress: (1) the applied uniformly distributed force parallel to the web, (2) the uniformly distributed force provided by the sheathing perpendicular to the web, and (3) the shear force generated by the torsion brace. As previously discussed, the force generated in the sheathing is directly proportional to the applied force parallel to the web of the purlin by the factor ρ. The stresses are mapped according to the modified moments of inertia as presented by Zetlin and Winter (1955). Because the shear forces generated by the torsion brace are equal and opposite, an axial force will be generated in the brace, balancing unsymmetric bending effects. Therefore, the stress distributions that result from the torsion brace shear forces will conform to the constrained bending distribution.

In the length of the purlin between the end of the purlin and the torsion brace, ie. $z \le c$, the bending stresses can be mapped by at coordinates x and y across the purlin cross section by

$$f_b = \frac{w(\cos\theta)L^2}{12}\left(6\left(\frac{z}{L}-\left(\frac{z}{L}\right)^2\right)-1\right)\left[\frac{-y}{I_{mx}}+\frac{x\frac{I_{xy}}{I_x}}{I_{my}}-\frac{x\cdot\rho}{I_{my}}+\frac{y\frac{I_{xy}}{I_y}\rho}{I_{mx}}\right]+ \\ +V_i\cdot L\left(\frac{z}{L}-\frac{c}{L}\left(1-\frac{c}{L}\right)\right)\left(\frac{-y}{I_x}\right) \quad (14)$$

Similarly, in the region of the purlin between the brace and mid-span, ie. $c \le z \le L/2$, the bending stresses can be mapped by .

$$f_b = \frac{w(\cos\theta)L^2}{12}\left(6\left(\frac{z}{L}-\left(\frac{z}{L}\right)^2\right)-1\right)\left[\frac{-y}{I_{mx}}+\frac{x\frac{I_{xy}}{I_x}}{I_{my}}-\frac{x\cdot\rho}{I_{my}}+\frac{y\frac{I_{xy}}{I_y}\rho}{I_{mx}}\right]+V_i\cdot\frac{c^2}{L}\left(\frac{-y}{I_x}\right) \quad (15)$$

Although the equations are generalized to calculate stresses at any location, for a uniformly distributed load, the critical locations to check stresses are the brace location, ie. z = c, and at mid-span, z = L/2.

Torsion stresses are superimposed on the bending stresses to get the net distribution of stresses. Warping torsion normal stresses, f_w are calculated as presented AISC Torsion Analysis Design Guide (Seaburg and Carter, 1997).

$$f_w = E \cdot W_N \cdot \phi'' \tag{16}$$

In Eq (16), W_N is the normalized warping function at a specific point on the cross section and ϕ'' is the second derivative of the rotation function for the applied load with respect to the z-axis along the span of the beam. At the critical stress locations (mid-span and brace location), rotation functions are derived for each torsion function acting on the purlin (uniform, parabolic, concentrated torque at braces).

At the mid-span location, the rotation functions are:

Uniform Torsion

$$\phi_u'' = \frac{t_{1st}}{GJ}\left(\left(\frac{L}{2a}\right)\frac{1}{\sinh\left(\frac{L}{a}\right)} - 1\right) \tag{17}$$

Parabolic Torsion

$$\phi_p'' = \frac{t_{2nd}}{GJ}\left[\frac{L}{a}\left(\frac{1}{3} - \frac{4a^2}{L^2}\right)\left(\frac{1}{\sinh\left(\frac{L}{2a}\right)}\right) + \frac{8a^2}{L^2} - 1\right] \tag{18}$$

Concentrated Brace Torsion

$$\phi_{brace}'' = \frac{T_{1st} + T_{2nd}}{GJ}\left(\frac{1}{a}\right)\left[\left(1 - \cosh\left(\frac{c}{a}\right)\right)\left(\frac{1}{\sinh\left(\frac{L}{2a}\right)}\right)\right] \tag{19}$$

At the brace location, the rotation functions are:

Uniform Torsion

$$\phi_u'' = \frac{t_{1st}}{GJ}\left(\left(\frac{L}{2a}\right)\left(\frac{\cosh\left(\frac{L}{2a}\right)}{\sinh\left(\frac{L}{2a}\right)}\right)\cosh\left(\frac{c}{a}\right) - \left(\frac{L}{2a}\right)\sinh\left(\frac{c}{a}\right) - 1\right) \tag{20}$$

Parabolic Torsion

$$\phi_p'' = \frac{t_{2nd}}{GJ}\left[\frac{L}{a}\left(\frac{1}{3} - \frac{4a^2}{L^2}\right)\left(\frac{\cosh\left(\frac{L}{2a}\right)}{\sinh\left(\frac{L}{2a}\right)}\cosh\left(\frac{c}{a}\right) - \sinh\left(\frac{c}{a}\right) + 1\right) + 4\left(\frac{c}{L}\right)^2 - 4\left(\frac{c}{L}\right) + \frac{8a^2}{L^2}\right] \tag{21}$$

Concentrated Brace Torsion

$$\phi_{brace}'' = \frac{T_{1st} + T_{2nd}}{GJ}\left(\frac{1}{a}\right)\left(1 - \cosh\left(\frac{c}{a}\right)\right)\left(\frac{\cosh\left(\frac{L}{2a}\right)}{\sinh\left(\frac{L}{2a}\right)}\cosh\left(\frac{c}{a}\right) - \sinh\left(\frac{c}{a}\right)\right) \tag{22}$$

Calculating local and distortional buckling strength

To evaluate the local and distortional buckling strength, a uniformly distributed force is applied to the purlin. Cross section stresses are calculated according to the previous section at critical locations along the span of the purlin. From the stress distribution, the peak stress, f_{max} is determined. The moment about the x-axis, M_x, that corresponds to the critical location is calculated. For example, the moment about the x-axis at the mid-span of the purlin is

$$M_{x,mid} = \frac{w(\cos\theta)L^2}{24} + (V_i)\frac{c^2}{L} \tag{23}$$

The cross section stresses are then scaled by a factor of F_y/f_{max} to equate the stresses to the point of first yield. In the same fashion, the moment about the x-axis is scaled by the same scale factor to determine the yield moment, M_y, for use in calculations. Using the scaled stress distribution, a finite strip buckling analysis is performed using CUFSM v.4.05 (Li and Schafer, 2010) to determine the local and distortional buckling load factors. The critical local and distortional buckling moments, $M_{cr\ell}$ and M_{crd}, respectively, are calculated as the product of the buckling load factor and the yield moment. The nominal local buckling moment, $M_{n\ell}$, is calculated according to AISI Specification (2016) Section F3.2 with $F_n = F_y$ and

the nominal distortional buckling moment, M_{nd}, is calculated according to AISI Section F4.1. The minimum of the local and distortional buckling moment is the nominal strength, M_n. which is then compared to the moment about the x-axis, M_x. If $M_n > M_x$, the purlin has sufficient capacity to support the uniform load. Because the methodology includes approximate second order effects, as long as $M_n > M_x$, second order effects have been over-estimated and the result is conservative. If the precise value of the maximum nominal moment that the purlin can sustain is desired, some iteration is required.

Predicted Strength of Sloped Roofs

The philosophy of the design of sloped roof systems has been to determine the strength of the purlin system in a flat roof condition using the base test and any slope effects are resisted by the anchorage system. The lateral deflection of the system is limited to L/360 for most systems and L/180 for torsion braces. While this approach is generally considered to be conservative, it is hypothesized that increased capacity can be realized by including slope effects to evaluate the actual strength. It is also desirable to relax lateral deflection limits, which is reasonable when the strength of the purlin directly incorporates the effects of lateral deformations.

To test this hypothesis, a system of purlins was evaluated on slopes varying from a 0:12 pitch to a 4:12 pitch. To provide a baseline for comparison, the system of purlins evaluated is derived from the system of base tests performed by Emde (2010). The same system of base tests was evaluated by Seek and Parva (2018) using a variation of the methodology presented in this paper with good correlation. From the series of tests, two purlins were evaluated: an 8ZS2.00x057 (Test ID 8Z16-1A) and an 8ZS2.00x100 (Test ID 8Z12-2D). The measured cross section dimensions reported by Emde were used. The purlin span, L = 27 feet, and the torsion braces are spaced at c = 10.5 feet from the ends. The diaphragm stiffness values were the same as used by Seek and Parva (2018), who calibrated diaphragm stiffness to measured deflections. Test parameters are summarized in Table 1.

Table 1. Purlin System Analysis Parameters

Purlin	F_y (ksi)	G' (lb/in)	standoff, s (in)	eccentricity, e_{sx} (in)
8Zx057	70.8	230	2.5	0.333
8Zx100	79.1	110	2.5	0.333

The relationship between the predicted maximum supported uniform load in the gravity direction and roof slope is shown Figure 3 for the 8Zx057 purlin and in Figure 4 for the 8Zx100 purlin. Maximum supported uniform load is used as a

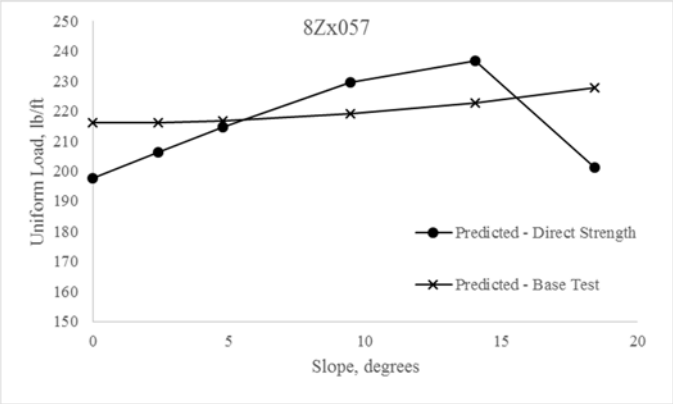

Figure 3. Maximum uniform load vs. roof slope, 8Zx057

comparison rather than the moment at failure because the moment at failure fluctuates considerably as a result of the brace shear. In both Fig 3 and Fig 4, the strength predicted by the R-factor derived from the base test is also plotted as a base line. The small increase in strength in the strength derived from the base test with increasing roof slope results from the subdivision of the gravity load into components perpendicular and parallel to the plane of the sheathing.

For the 8Zx057 purlin, at the flat roof condition, the strength predicted from the Direct Strength Method is slightly less than that predicted by Base Test Method. The relatively large lateral deflection results in biaxial bending stresses that increase the web stresses and cause local buckling of the web. In Table 2, the calculated local and distortional buckling load factors at both the mid-span and brace location are provided, as well as the predicted maximum supported load predicted from the buckling load factors with the controlling load highlighted. Table 2 also reports the uniform load equivalent to the base test R-factor as well as the predicted buckling load factors from the base test for comparison to the sloped multi-span system results. Table 3 presents the stress scale factors, predicted failure mode and location, as well as the lateral deflection of the system.

As the slope of the roof system increases, and the downslope component of the gravity load begins to contribute downslope forces to the diaphragm, the lateral deflection of the purlins decreases. Correspondingly, the brace moments decrease as second order torsion decreases and the stress scale factor increases, indicating the redistribution of stresses away from the web. The supported uniform load increases as a result of the change in distribution of stresses. With increasing slopes, the failure mode changes. At slopes higher than a 3:12 pitch, the lateral deflection of the purlin transitions downslope. The lateral bending effect in this

case shifts stresses towards the flange tips. The combination of lateral bending and concentrated torsion at the brace location cause the failure mode to shift to local buckling of the flange stiffener at the brace location. This shift in stresses causes the supported uniform load to rapidly decline. However, in this case, peak stresses occur in the tension flange, so additional strength may be realized by considering inelastic reserve capacity.

Table 2: Buckling load factors and maximum uniform loads for 8Zx057 purlin

	Buckling Load Factors				Uniform Load (lb/ft)				
	Mid-span		Brace		Mid-span		Brace		Min.
	Local	Dist.	Local	Dist.	Local	Dist.	Local	Dist.	
Base Test	0.60	0.67	0.62	0.66	-	-	-	-	216
0:12	0.59	1.02	0.92	0.83	198	218	230	203	198
0.5:12	0.59	0.93	0.85	0.78	206	220	242	214	206
1:12	0.58	0.85	0.78	0.74	215	223	255	227	215
2:12	0.58	0.71	0.61	0.67	237	230	285	266	230
3:12	0.58	0.59	0.52	0.82	262	237	241	257	237
4:12	0.70	0.59	0.63	1.00	261	221	201	216	201

Table 3. Analysis comparisons 8Zx057 purlin

			Failure				Deflection	
	Max w_n (lb/ft)	F_n/F_y	Up/Down	Location	Mode	Brace Moment (lb-ft)	Lateral (in)	Ratio L/
Base Test	216	1.457	Downhill	Mid	Dist.	387	1.86	174
0:12	198	1.406	Uphill	Mid	Local	2935	2.78	117
0.5:12	206	1.406	Uphill	Mid	Local	2474	2.45	132
1:12	215	1.414	Uphill	Mid	Local	1895	2.09	155
2:12	230	1.457	Uphill	Mid	Dist.	305	1.24	260
3:12	237	1.578	Uphill	Mid	Dist.	-1529	0.28	1166
4:12	201	1.374	Downhill	Brace	Local	-2675	-0.59	553

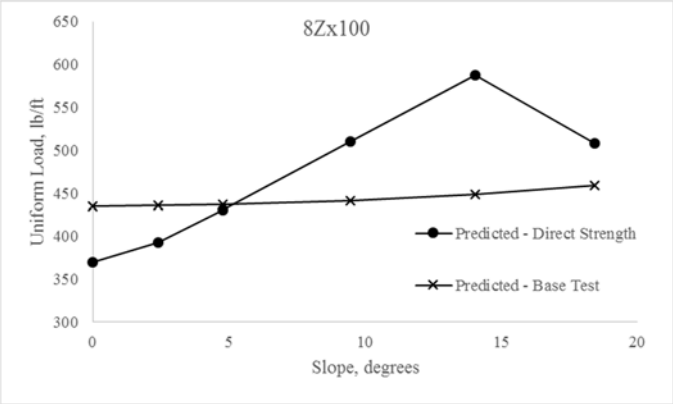

Figure 4. Maximum uniform load vs. roof slope, 8Zx100

The relationship between the roof slope and the supported uniform load as shown in Fig. 4 for 8Zx100 is similar to that of the 8Zx057 purlin. At the flat slope, the strength predicted by the direct strength method is less than that predicted by base test R-factor. With increasing slope, the strength predicted by direct strength method increases with a maximum at a pitch of approximately 3:12, then begins to dramatically decrease. Although the overall trends between the thicker and thinner purlin are similar, the predicted behavior as summarized in Table 4 and 5 for the 8Zx100 purlin is different. For the thicker purlin, the large lateral deflections cause substantial second order torsions which causes large torsion brace moments. The predicted failure mode is distortional buckling at the brace location.

Table 4: Buckling load factors and maximum uniform loads for 8Zx100 purlin

	Buckling Load Factors				Uniform Load (lb/ft)				Min.
	Mid-span		Brace		Mid-span		Brace		
	Local	Dist.	Local	Dist.	Local	Dist.	Local	Dist.	
Base Test	1.72	1.90	2.54	1.52	-	-	-	-	435
0:12	1.59	N/A	3.21	2.07	437	N/A	376	370	370
0.5:12	1.59	3.5	3.1	1.86	466	472	412	393	393
1:12	1.58	2.43	2.83	1.7	498	506	464	431	431
2:12	1.57	1.74	2.41	1.35	581	553	590	511	511
3:12	1.55	1.18	1.57	1.16	696	588	824	689	588
4:12	1.94	1.02	1.73	1.88	692	543	530	508	508

Table 5: Analysis comparisons 8Zx100 purlin

	Max w_n (lb/ft)	F_n/F_y	Failure			Brace Moment (lb-ft)	Deflection	
			Up/Down	Location	Mode		Lateral (in)	Ratio L/
Base Test	435	1.105	Uphill	Brace	Dist.	5362	6.17	53
0:12	370	1.017	Uphill	Brace	Dist.	13777	5.44	60
0.5:12	393	1.048	Uphill	Brace	Dist.	12977	4.95	65
1:12	431	1.075	Uphill	Brace	Dist.	11419	4.30	75
2:12	511	1.156	Uphill	Brace	Dist.	8541	3.30	98
3:12	588	1.210	Downhill	Mid-	Dist.	-28	1.21	268
4:12	508	1.044	Downhill	Brace	Dist.	-8796	-1.00	323

As the slope increases, the second order torsion decreases and the predicted supported uniform load increases. Similar to the thinner purlin, as the lateral deflection of the purlin transitions downslope at pitches greater than 3:12, the predicted strength decreases. As for the thin purlin, the tension stresses are significantly higher than the compression stresses, so additional strength can likely be realized by considering inelastic reserve capacity.

Conclusions

A method is presented to predict the local and distortional buckling strength of purlins with one flange attached to standing seam sheathing and braced by paired torsion braces using the Direct Strength Method. The methodology uses displacement compatibility between the purlin, sheathing, and braces, to calculate the actual stress distribution of the stresses in the cross section. With the inclusion of roof slope, the distribution of stresses can change significantly, which changes the predicted load carrying capacity, failure mode and failure location. The presented method, which conservatively ignores the additional strength from the torsional restraint provided by the sheathing, predicts strength slightly less than the base test at low slopes and greater strength at higher slopes. Therefore, the presented method may not only be replacement to base test method, but it may allow for increases in strength at certain roof slopes. Additionally, the presented method links the strength of the purlin directly to the restraint provided by the sheathing and the deformation of the system. In most cases, although the lateral deflection falls outside the limits allowed by the AISI Specification, the purlin does not experience a loss in strength until the lateral deflection shifts downslope. Therefore, the presented method provides evidence that the AISI lateral deflection

limits may be relaxed provided that the second order effects caused by lateral deflection in incorporated into the analysis.

References

American Iron and Steel Institute (AISI) (2016). *AISI S100-16 North American Specification for the Design of Cold-Formed Steel Structural Members*. Washington, DC. 2016.

American Iron and Steel Institute (AISI) (2013). *S908-13 Base Test Method for Purlins Supporting a Standing Seam Roof System*. AISI. Washington, DC. 2013.

Emde, M. G. (2010) Investigation of Torsional Bracing off Cold-Formed Steel Roofing Systems. *Master's Thesis*. University of Oklahoma. Norman, OK. 2010.

Li, A., Schafer, B.W. (2010) "Buckling analysis of cold-formed steel members with general boundary conditions using CUFSM: conventional and constrained finite strip methods." *Proceedings of the 20th International Specialty Conference on Cold-Formed Steel Structures*. 2010.

Parva, A. and Seek, M.W. (2018). "Direct Strength Approach to Predict the Flexural Strength of Cold-Formed Z-Section Purlins on Sloped Roofs" *Conference Proceedings, SSRC Annual Stability Conference*. Structural Stability Research Council, University of Missouri-Rolla, Rolla, Missouri. 2018

Seaburg, P. A., Carter, C. J. (1997) *Steel Design Guide Series 9: Torsional Analysis of Structural Steel Members*. American Institute of Steel Construction. Chicago, IL. 1997.

Seek, M.W., Ramseyer, C. and Kaplan, I. (2016). "A Combined Direct Analysis and Direct Strength Approach to Predict the Flexural Strength of Z-Purlins with Paired Torsion Braces". *Proceedings of the 23rd International Specialty Conference on Cold-Formed Steel Structures*. 2016.

Seek, M.W., and Parva, A. (2018). "Predicting the Strength of Z-section purlins with One Flange Attached to Standing Seam Sheathing Using the Direct Strength Method". *Eighth International Conference on THIN-WALLED STRUCTURES – ICTWS 2018*. Lisbon, Portugal, July 24-27, 2018.

Zetlin, L and G. Winter. (1955). "Unsymmetrical Bending of Beams with and without Lateral Bracing." *Journal of the Structural Division*, ASCE, Vol. 81, 1955.